

Contactless Inductive Flow Tomography: A Liquid Metal Flow Measuring Technique Complementary to UDV

Frank Stefani, Gunter Gerbeth, Thomas Gundrum, and Thomas Wondrak
Helmholtz-Zentrum Dresden-Rossendorf, P.O. Box 510119, D-01314 Dresden, Germany

The aim of the Contactless Inductive Flow Tomography (CIFT) is the reconstruction of flow structures in metal and semiconductor melts. It relies on the induction of electric currents in moving conductors exposed to magnetic fields. The flow induced deformations of various applied magnetic fields can be measured in the exterior of the melt and utilized for the reconstruction of the velocity field. After a presentation of the principles of CIFT, first applications and possible extensions of the method are discussed and put into the context with traditional measuring techniques such as UDV.

Keywords: Contactless inductive flow tomography, Steel casting, Crystal growth

1 INTRODUCTION

Ultrasound Doppler Velocimetry (UDV) is nowadays the most appropriate measuring technique when it comes to flow field determinations in opaque fluids for which optical methods like Particle Image Velocimetry (PIV) or Laser Doppler Velocimetry (LDV) are not applicable. Since the pioneering work of Takeda [1], UDV has been established as a standard technique for flow field determinations in liquid metals, in particular. Great effort is presently being spent on extending the range of UDV to higher-dimensional flow mappings [2], and to high temperature applications by the use of waveguides between the transducer and the liquid [3].

Yet, there are some particular measuring tasks for which the application of UDV is hard to imagine. One example is the casting of steel which works at temperatures around 1500°C. Another one is the growth of silicon mono-crystals in the Czochralski process in which the use of UDV is not only prevented by the high temperatures (around 1400°C) but also by the demand that the silicon melt must be clean and free of any tracer particles. Hence, for those technologies there is an urgent need for alternative flow measuring techniques. Fortunately, most of the hot fluids to be monitored are liquid metals or liquid semiconductors, both characterized by a relatively high electrical conductivity in the order of 10^6 S/m. The movement of such good electrical conductors under the influence of externally applied magnetic field is known to induce electrical currents which are, in turn, the source of induced magnetic fields. When measuring these flow induced magnetic fields in the exterior of the melt, one can try to extract information about the velocity field. This is the basic idea of the Contactless Inductive Flow Tomography (CIFT), to be discussed in this paper.

2 BASIC THEORY

When an electrically conducting medium, moving with the velocity \mathbf{u} , comes under the influence of a

magnetic field \mathbf{B} , an electromotive force (emf) $\mathbf{u} \times \mathbf{B}$ is induced that drives an electric current with density

$$\mathbf{j} = \sigma(\mathbf{E} + \mathbf{u} \times \mathbf{B}), \quad (1)$$

where σ is the electrical conductivity of the melt and \mathbf{E} is the electric field. In the stationary case, we can express \mathbf{E} in terms of the gradient of the electric potential, $\mathbf{E} = -\nabla\phi$. Then, Biot-Savart's law gives the following expression for the induced magnetic field \mathbf{b} :

$$\begin{aligned} \mathbf{b}(\mathbf{r}) = & \frac{\sigma\mu_0}{4\pi} \int_D \frac{(\mathbf{u}(\mathbf{r}') \times \mathbf{B}(\mathbf{r}')) \times (\mathbf{r} - \mathbf{r}')}{|\mathbf{r} - \mathbf{r}'|^3} dV' \\ & - \frac{\sigma\mu_0}{4\pi} \iint_S \phi(\mathbf{s}') d\mathbf{S}' \times \frac{\mathbf{r} - \mathbf{s}'}{|\mathbf{r} - \mathbf{s}'|^3}. \end{aligned} \quad (2)$$

Note that the surface integral term on the left hand side of Eq. (2) results from converting an equivalent volume integral with $\nabla\phi$ in the integrand. Note further that this term must not be neglected (as was done, e.g., in earlier attempts for a magnetic flow tomography [4]), since it can attain the same order of magnitude as the first term, possibly cancelling it completely for special flow and magnetic field configurations. By applying the divergence operator to Eq. (1) we obtain the Poisson equation for the electric potential, $\Delta\phi = \text{div}(\mathbf{u} \times \mathbf{B})$, whose solution can be shown to fulfill the boundary integral equation

$$\begin{aligned} \phi(\mathbf{s}) = & \frac{1}{2\pi} \int_D \frac{(\mathbf{u}(\mathbf{r}') \times \mathbf{B}(\mathbf{r}')) \cdot (\mathbf{s} - \mathbf{r}')}{|\mathbf{s} - \mathbf{r}'|^3} dV' \\ & - \frac{1}{2\pi} \iint_S \phi(\mathbf{s}') d\mathbf{S}' \cdot \frac{\mathbf{s} - \mathbf{s}'}{|\mathbf{s} - \mathbf{s}'|^3}. \end{aligned} \quad (3)$$

The two integral equations (2) and (3) are valid for rather general induction processes, and can also be employed to solve dynamo problems in which a magnetic field self-excites under the influence of a velocity field, without applying any external magnetic field. For many industrial problems, however, the ratio of the induced field \mathbf{b} to an externally applied field \mathbf{B}_0 is typically smaller than one, so that the total

field $\mathbf{B} = \mathbf{B}_0 + \mathbf{b}$ under the integrals in Eqs. (2) and (3) can be replaced by the applied magnetic field \mathbf{B}_0 alone. It is this replacement that makes the inverse problem of reconstructing the velocity field from the induced electro-magnetic fields a linear one, which is much easier solvable than the full-fledged nonlinear problem with $\mathbf{B}_0 + \mathbf{b}$ under the integrals.

In a very first attempt [5,6] we had shown that, with a vertical field $\mathbf{B}_{0,z}$ being applied, the velocity structure of the flow can be roughly reconstructed from the external measurement of the induced magnetic field in the exterior and of the induced electric potential at the boundary of the fluid. There remains, however, a non-uniqueness concerning the exact radial distribution of the flow, a fact that can be made plausible by representing the fluid velocity by two defining scalars (for the poloidal and the toroidal velocity component), living both in the whole fluid volume. Then it is clear that two quantities measured only on a two-dimensional covering of the fluid cannot give enough information for the reconstruction of the two desired 3D-quantities.

Later, then, we had developed a completely contactless method, CIIFT, to avoid the electric potential measurement at the fluid boundary [7]. The main idea was to apply the external magnetic field in two different, e.g. orthogonal, directions and to utilize both corresponding sets of induced magnetic fields for the velocity field reconstruction.

3 A FIRST DEMONSTRATION EXPERIMENT

The goal of a first demonstration experiment [8] for CIIFT was the reconstruction of a propeller-driven three-dimensional flow of the eutectic alloy GalnSn in a compact cylindrical vessel with a ratio of height to diameter close to one (Fig. 1). In order to determine both the poloidal (in r and z) and the toroidal (in ϕ) flow component, we applied subsequently a vertical ($\mathbf{B}_{0,z}$) and a horizontal ($\mathbf{B}_{0,x}$) magnetic field, either produced by Helmholtz-like coil pairs. In this experiment, the switching between the two fields occurs every 3 seconds, so that after 6 seconds all the magnetic field information is available for the velocity reconstruction. Note that, in principle, this rather poor time resolution can be significantly enhanced, with a physical limitation given by the magnetic decay time $\mu_0 \sigma R^2$, which is in the order of 0.05 s for the demonstration experiment.

For each of the two applied fields, $\mathbf{B}_{0,z}$ and $\mathbf{B}_{0,x}$, the induced fields are measured by Hall sensors at 48 positions, which are rather homogeneously distributed all around the surface of the cylindrical vessel. The rather small ratio of around $10^3 \dots 10^2$, between the induced and the applied fields, demands for a very stable current source of the Helmholtz-like coils, for a very stable relative position of Hall sensors and coils, and for significant effort to compensate drift and sensitivity changes of

the Hall sensors (e.g., due to varying temperature).

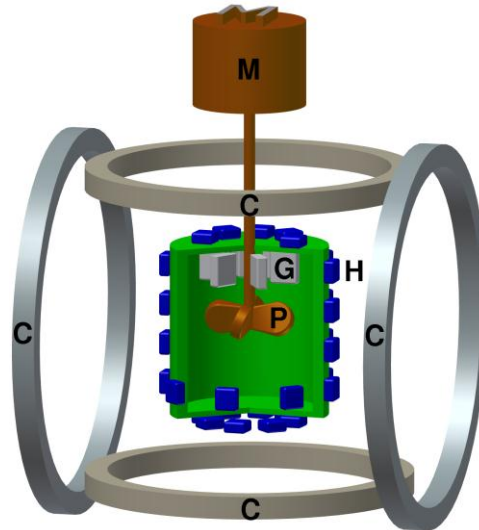


Figure 1: Schematic sketch of the demonstration experiment for the validation of CIIFT at a propeller-driven 3D flow of GalnSn. M - Motor, C - Coils, P - Propeller, G - Guiding blades, H - Hall sensors.

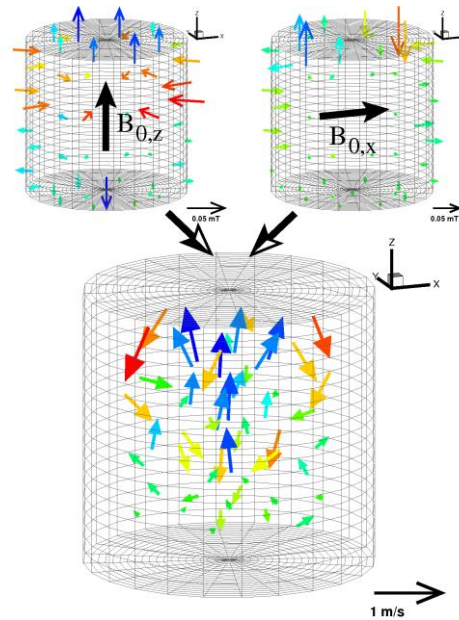


Figure 2: Velocity field for upward pumping (below), as reconstructed by the externally measured induced magnetic fields for applied $\mathbf{B}_{0,z}$ and $\mathbf{B}_{0,x}$ (above). The color scale of the induced fields indicates the normal component relative to the nearest surface point, the color scale of the velocity vectors indicates the z -component.

For the reconstruction of the velocity field we solve the Gauss normal equations that minimize the mean quadratic deviation of the measured from the modeled induced magnetic fields. The intrinsic non-uniqueness problem concerning the detailed depth-dependence of the velocity is overcome by utilizing the so-called Tikhonov regularization by minimizing,

in parallel to the magnetic field deviations, also the kinetic energy of the flow or other appropriate quadratic functionals of the velocity. This numerical scheme can easily be extended to incorporate further a-priori information, e.g. the divergence-free condition of the velocity field, or velocity components and mass flow rates known from other measuring techniques.

In this experiment it was possible to distinguish clearly between upward and downward pumping of the propeller, with the rotational component being reduced by guiding blades in the case of upward pumping. For the latter case, Fig. 2 shows the induced fields for applied $\mathbf{B}_{0,z}$ und $\mathbf{B}_{0,x}$, respectively, and the velocity field as reconstructed from this information. The comparison with UDV measurements has shown a good coincidence of the resulting velocity fields (see [8]).

3 APPLICATION TO CONTINUOUS CASTING PROBLEMS

In the continuous casting of steel, the liquid metal flows from a tundish through a Submerged Entry Nozzle (SEN), with typically two ports at the lower end, into the mould where it starts to solidify at the water-cooled copper walls. The quality of the produced steel depends critically on the detailed flow structure in the mould. What is desirable here is a so-called double-roll structure, with the two jets that emanate from the SEN ports first reaching the narrow-faces of the mould and then splitting into upward and downward directed branches. In contrast to that, the so-called single-roll structure, with the jets being sharply bent upward after leaving the SEN ports, is considered dangerous since it could lead to entrainment of casting powder into the steel.

Any sort of online-monitoring of the detailed roll-structure in the mould would allow for an active control of the casting process, with the prospect to increase the possible casting speed significantly. As a contactless method, CIFT suggests itself for such monitoring, although the problem of the copper-mould oscillations makes its implementation in the industry still a formidable task. As a first step in this direction, we have installed a simplified CIFT system at our small continuous casting model Mini-LIMMCAST, working also with the GaInSn alloy [9]. The simplification concerns the restriction of the CIFT system to only one magnetic field coil which produced a mainly vertical magnetic field. This configuration is sufficient for the determination of the velocity component parallel to the wide faces of the mould [10], which is the dominant one for the slab-casting as modeled in Mini-LIMMCAST. The induced fields are now measured by Fluxgate sensors positioned at the narrow faces of the mould, typically at 7-9 positions on either side.

In addition to CIFT, we have utilized a Mutual

Inductance Tomography (MIT) system for determining the conductivity distribution in the SEN, which allows visualizing the details of the two-phase GaInSn/Argon flow. The simultaneous utilization of CIFT and MIT leads to a detailed understanding of the two-phase flow in the SEN and of the resulting flow in the mould [11]. Figure 4 illustrates various flow structures that had been detected during one run of the experiment, including double-roll and single roll structures occurring on different sides of the mould.

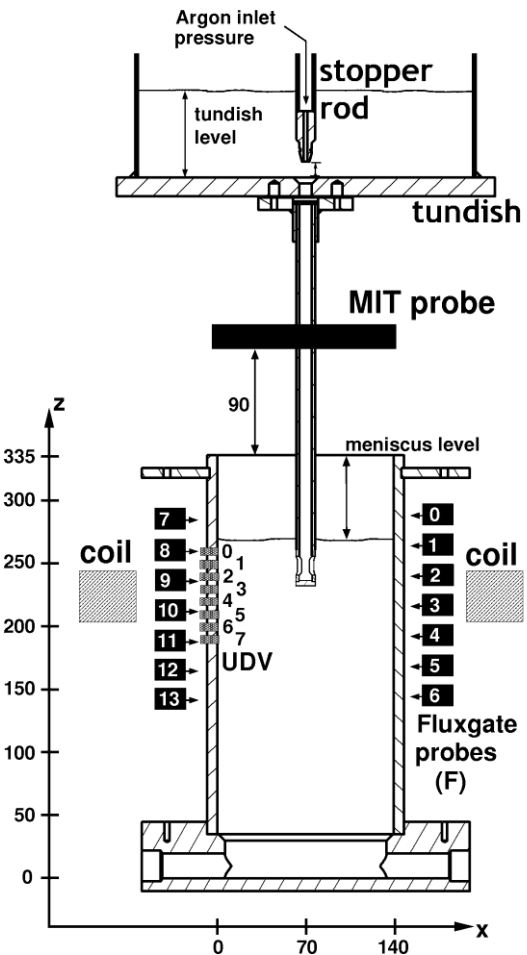


Figure 3: Schematic sketch of the Mini-LIMMCAST facility and the employed CIFT, UDV and MIT technique. The use of one coil is sufficient for the reconstruction of the basically 2-dimensional flow field in the mould. Lengths are in mm.

It might be interesting to see, in particular for the audience of the ISUD workshop, how CIFT compares with traditional UDV measurements. For this purpose, we show in Fig. 5 the x-component of the velocity as determined both by CIFT and UDV at a height of $z=210$ mm over the course of one run. Despite some slight quantitative differences, the general agreement between the two results is quite convincing.

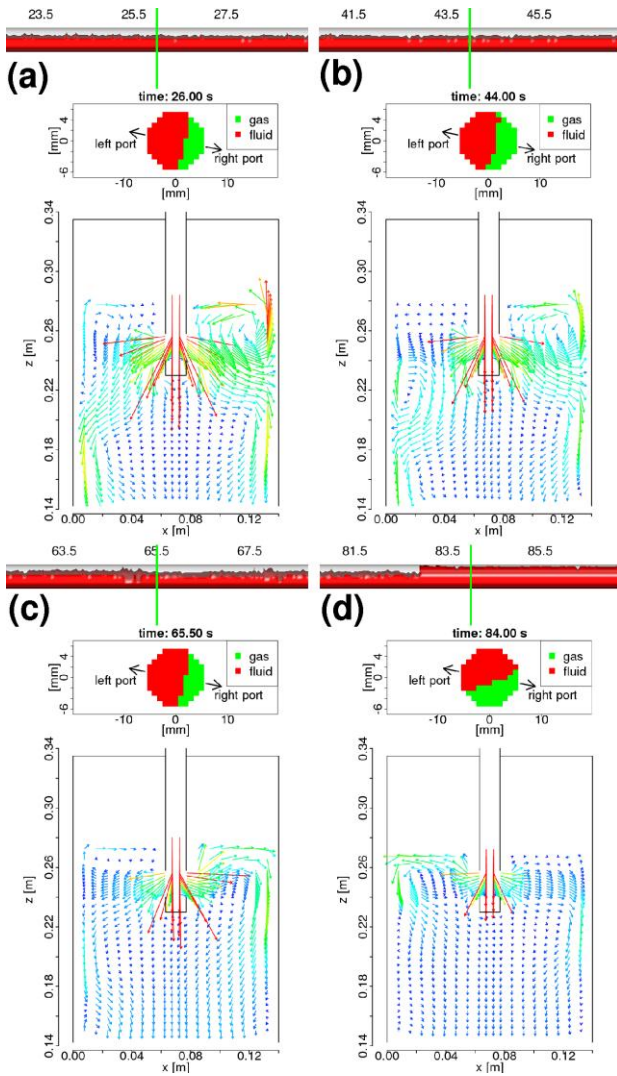


Fig. 4. CIFT reconstructed velocity in the mould , and MIT reconstructed metal distribution in the SEN at four instants (a - 26 s; b - 44 s; c - 65.5 s; d - 84 s) during one two-phase experiment with an argon flow rate of $500 \text{ cm}^3/\text{min}$. Different flow structures (a,b – double roll, c,d – single roll on different sides) are clearly visible.

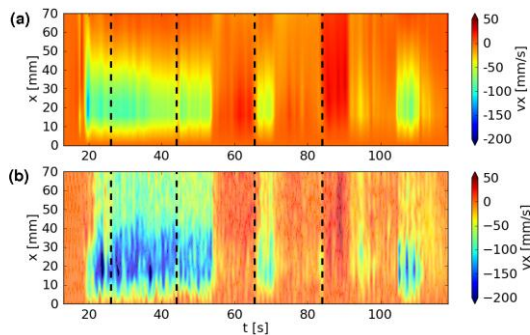


Figure 5: Comparison of the CIFT reconstructed (a) and the UDV determined (b) v_x component at $z = 210 \text{ mm}$ in dependence on time and x -coordinate. The dashed lines indicate the snapshots illustrated in Fig. 4.

6 SUMMARY AND OUTLOOK

In this paper, we have summarized the recent efforts in the development of the Contactless Inductive Flow Tomography, and put them into the context of established flow measurement techniques like UDV. While CIFT, as a global reconstruction technique with an intrinsic non-uniqueness, will never attain the precision of UDV measurement, the avoidance of any contact with the melt makes it promising for some special measurement tasks in very hot and/or chemically aggressive and/or extremely clean metallic and semiconducting melts. Presently, work is going on to make the method more robust (by using AC measuring fields and gradiometric coils) for its envisioned industrial deployment.

REFERENCES

- [1] Takeda Y: Measurement of velocity profile of mercury flow by ultrasound Doppler shift method, Nucl. Technol. 79 (1987), 120-124.
- [2] Franke S et al.: Ultrasound Doppler system for two-dimensional flow mapping in liquid metals, Flow Meas. Instrum. 21 (2010), 402-409.
- [3] Eckert S et al.: Velocity measurement techniques for liquid metal flows, In: S. Molokov, R. Moreau, H.K. Moffatt (eds.) Magnetohydrodynamics – Historical Evolution and Trends, Springer (2007), pp. 275-294.
- [4] Baumgartl J et al.: The use of magnetohydrodynamic effects to investigate fluid flow in electrically conducting melts, Phys. Fluids A 5 (1993), 3280-3289.
- [5] Stefani F and Gerbeth G: Velocity reconstruction in conducting fluids from magnetic field and electric potential measurements, Inverse Problems 15 (1999), 771–786.
- [6] Stefani F and Gerbeth G: On the uniqueness of velocity reconstruction in conducting fluids from measurements of induced electromagnetic fields, Inverse Problems 16 (2000), 1–9.
- [7] Stefani F and Gerbeth G: A contactless method for velocity reconstruction in electrically conducting fluids, Meas. Sci. Techn. 11 (2000), 758–765.
- [8] Stefani F et al.: Contactless inductive flow tomography, Phys. Rev. E. 70 (2004), 056306.
- [9] Timmel K et al.: Experimental modeling of the continuous casting process of steel using low melting point alloys - the LIMMCAST program, ISIJ International 50 (2010), 1134-1141.
- [10] Wondrak T et al.: Contactless inductive flow tomography for a model of continuous steel casting, Meas. Sci. Techn. 21 (2010), 045402.
- [11] Wondrak T et al.: Combined electromagnetic tomography for determining two-phase flow characteristics in the submerged entry nozzle and in the mould of a continuous-casting model, Met. Mat. Trans. B 42 (2011), 1201-1210.